Translational Oncology 15 (2022) 101282

Contents lists available at ScienceDirect

Translational Oncology

journal homepage: www.elsevier.com/locate/tranon

Original Research

LncRNA RBPMS-AS1 promotes NRGN transcription to enhance the radiosensitivity of glioblastoma through the microRNA-301a-3p/CAMTA1 axis

Wenyang Li [a], Yan Cui [a], Wenjia Ma [a], Ming Wang [a], Yang Cai [a], Yugang Jiang [a,*]

[a] Department of Neurosurgery, Second Xiangya Hospital of Central South University, Changsha, Hunan 410011, PR China

ARTICLE INFO

Keywords:
Glioblastoma
LncRNA RBPMS-AS1
microRNA-301a-3p
CAMTA1
NRGN
Radiosensitivity

ABSTRACT

Objective: Glioblastoma (GBM) is the most frequent brain malignancy with high incidence, and long noncoding RNAs (lncRNAs) exerts functions in GBM. In this research, we focused on the capabilities of lncRNA RBPMS-AS1 in radiosensitivity of GBM.

Methods: RBPMS-AS1 and CAMTA1 expression levels were determined in GBM tissues and cells. StarBase v3.0 database was searched for predicting miRNAs that simultaneously bound to RBPMS-AS1 and CAMTA1. pcDNA3.1-RBPMS-AS1, pcDNA3.1-CAMTA1, miR-301a-3p mimic, or pcDNA3.1-RBPMS-AS1/pcDNA3.1-CAMTA1 and miR-301a-3p mimic were transfected into GBM cells to test radiosensitivity, cell proliferation and apoptosis. The interactions of miR-301a-3p with RBPMS-AS1 and CAMTA1, as well as CAMTA1 and NRGN, were confirmed. In vivo imaging technology was utilized to detect tumor growth in orthotopic xenograft tumors, and Ki67 expression was tested in intracranial tumors.

Results: RBPMS-AS1 and CAMTA1 levels were reduced in GBM tissues and cells. miR-301a-3p had a binding site with both RBPMS-AS1 and CAMTA1 and it was the most significantly-upregulated one. Upregulation of RBPMS-AS1 or CAMTA1 enhanced the radiosensitivity and cell apoptosis while suppressing proliferation of GBM cells. Conversely, miR-301a-3p overexpression diminished the radiosensitivity and cell apoptosis while inducing proliferation of GBM cells. Overexpression of RBPMS-AS1 or CAMTA1 reversed the effects of overexpressed miR-301a-3p in GBM cells. Mechanistically, RBPMS-AS1 enhanced CAMTA1 expression in GBM cells through sponging miR-301a-3p, and CAMTA1 promoted NRGN expression. In animal experiments, overexpressed RBPMS-AS1 inhibited tumor growth and the positive expression of Ki67 both before and after radiation therapy.

Conclusion: RBPMS-AS1 promotes NRGN transcription through the miR-301a-3p/CAMTA1 axis and enhances the radiosensitivity of GBM.

Introduction

Glioblastoma (GBM) is the most frequent and aggressive type of primary malignant tumor in the central nervous system [1]. This disease is identified with specific characteristics of diffuse infiltration and local invasion into the surrounding brain tissues, significant cellular proliferation, robust angiogenesis, genomic instability, resistance to apoptosis, as well as a tendency for necrogenesis [2]. At present, considerable studies in GBM therapeutics are intended to develop vaccines or drugs so as to target the pivotal molecules for preventing this disease [3]. The prognosis for GBM patients remains grim even with significant advances in imaging methods, surgical techniques, achievements in radiation medicine, enhancing availability of targeted drugs and chemotherapeutics, as well as better understanding of the tumor biology [4]. For this regard, although GBM is a relatively rare type of cancer in terms of its incidence, it has disproportionately high ratios of cancer-related mortality and morbidity [5]. Thus, a clear unmet need is significant to improve the outcome and radiosensitivity for GBM patients.

Long noncoding RNAs (lncRNAs) modulate diverse oncogenes and tumor suppressor genes from the aspect of translation, transcription, protein localization, and function [6]. Additionally, lncRNAs are also

* Corresponding author at: Department of Neurosurgery, Second Xiangya Hospital of Central South University, No. 139, Mid Renmin Road, Furong District, Changsha, Hunan, 410011, PR China.
E-mail address: 198202108@csu.edu.cn (Y. Jiang).

https://doi.org/10.1016/j.tranon.2021.101282
Received 4 August 2021; Received in revised form 4 November 2021; Accepted 5 November 2021

implicated in the epigenetic control of DNA repair, cell differentiation and apoptosis [7, 8]. Recently, the abnormal expression of lncRNAs could play a role in the biological functions of human tumors, including glioma [9, 10]. The exploration of lncRNAs is essential for diagnosis and treatment of GBM. Evidence has shown that lncRNA RBPMS-AS1 is involved in the process of lung adenocarcinoma (LUAD) and cervical cancer [11, 12]. Yet, the specific actions of RBPMS-AS1 in GBM cells still needs further exploration. In the past several years, lncRNAs have been disclosed as competing endogenous RNAs (ceRNAs) to control mRNA expression via competitively sequestering certain miRs in many human cancers [13]. miRs are transcribed from DNA and participate in gene expression regulation in the small RNA molecule form [14]. Evidence has highlighted that the deregulation of miRs contributes to chemoresistance in cancers [15]. Previously, several articles have demonstrated that miR-301a-3p is an onco-miR in many types of cancers, such as breast cancer [16], stomach cancer [17], and pancreatic cancer [18]. Especially, miR-301a-3p has been also found in the development of glioma [19], but how miR-301a-3p is involved in glioma progression remains undetermined. Calmodulin-binding transcription activator 1 (CAMTA1) belongs to a recently-characterized protein family which is designated as calmodulin-binding transcription activators [20]. CAMTA1 is homozygously deleted in gliomas [21, 22] and is the only gene within the smallest region of overlap at 1p36 in this entity [23]. In a previous study, CAMTA1 was found to be regulated by miR-17 and miR-9/9(*) in glioblastoma stem cells [24]. Moreover, it has also been previously reported that NRGN is lowly expressed in GBM [25], and it is positively regulated by LINC00641 in GBM [26]. Based on the aforementioned evidences, this study was conducted to elucidate the functions of the RBPMS-AS1/miR-301a-3p/CAMTA1/NRGN axis in the progression and radiosensitivity of GBM.

Materials and methods

Ethics statement

Written informed consents were acquired from all patients before experiments. The protocol of this research was confirmed by the Ethics Committee of Second Xiangya Hospital of Central South University and based on the ethical principles for medical research involving human subjects of the *Helsinki Declaration*. Additionally, the animal experiment got the approval of the animal ethics committee of Second Xiangya Hospital of Central South University. All animal experiments abide by the rules, regulations and operational specifications of experimental animal management and related ethical requirements for experimental animals.

Patients and clinical samples

The paired GBM tissues and corresponding normal tissues were harvested from 38 patients who had been confirmed with primary GBM in Second Xiangya Hospital of Central South University between October 2016 and June 2019. Those patients who received radiotherapy or chemotherapy before surgery were excluded from our study.

Cell culture and irradiation

Four GBM cell lines (U251, U87, LN229 and A172) and normal human astrocytes (NHA) were available from Shanghai Institute of Biochemistry and Cell Biology, Chinese Academy of Sciences (Shanghai, China). GBM and NHA cells were cultured in Dulbecco's modified Eagle's medium (DMEM) supplemented with 10% fetal bovine serum in an incubator at 37℃ with 5% CO_2. For irradiation, U251 and U87 cells were seeded onto a 100-mm culture dishes at 1×10^6 cells per dish and then cultured for 24 h, before irradiation at room temperature with 0, 2, 4, 6 and 8 Gy laboratory X-ray by an irradiation apparatus (2100 C/D, VARIAN, CA, USA).

Cell transfection

Before transfection, GBM cells were placed in a 96-well plate. RBPMS-AS1 and CAMTA1 were amplified by polymerase chain reaction (PCR) and inserted into an empty vector (pcDNA3.1, Invitrogen, Carlsbad, CA, USA) to construct pcDNA3.1/RBPMS-AS1 and pcDNA3.1/CAMTA1 vectors. The pcDNA3.1/RBPMS-AS1 (2 μg), pcDNA3.1/CAMTA1 (2 μg), and miR-301a-3p mimic (100 nmol) were transfected into U87 and U251 cells, respectively. The cells were cultured in the 96-well plates until the cell confluence reached 70%−80%, and then transfected as per the protocols of Lipofectamine 2000. The cells upon 48 h transfection were collected for subsequent experiments.

3-[4,5-dimethylthiazol-2-yl]−2,5-diphenyl tetrazolium bromide (MTT) assay

U87 and U251 cells were exposed to 0, 2, 4, 6 and 8 Gy of X-ray irradiation, and the transfected cells were seeded onto a 96-well plate at 4000 cells per well. MTT assay was implemented for assessing the cell viability referring to the product instructions. In short, phosphate buffered saline (PBS) in each well was appended with 10 μL of 5 mg/mL MTT reagent and then incubated for 4 h at 37 °C. Afterwards, each well was supplemented with 150 μL of dimethylsulfoxide to dissolve the precipitate. Lastly, the measurement of the optical density (OD) value was carried out with a microplate reader at 490 nm.

Colony formation assay

The colony formation assay was implemented for evaluating the cell proliferation in different groups. In brief, the cells after transfection were seeded onto a 6-well plate, irradiated with 6 Gy, and then cultured for 10 days. More than fifty naturally-formed colonies were subjected to fixing with 75% ethanol and staining with 0.5% (w/v) crystal violet solution (Sigma-Aldrich, St. Louis, MO, USA), followed by the observation of the number of colonies by using a microscope (Wetzlar, Leica Microsystems, Germany), and photographing by a digital camera and analyzing by an Image J 2.0 version software.

Flow cytometry

The cell apoptosis was determined by Annexin V/propidium iodide (PI) Apoptosis Detection Kit (KeyGEN Biotech, Nanjing, China). In short, the transfected cells were seeded onto a 6-well plate and irradiated with 6 Gy, washed once with pre-cooled PBS, and added with 300 μL of 1×binding buffer to suspend the cells. Subsequently, the cells were appended with 5 μL of Annexin V-fluoresceine isothiocyanate solution and 5 μL of PI solution, and reacted for 15 min in darkness. After passing through a 300-mesh sieve, the cell apoptosis was tested on a flow cytometer (Becton Dickinson; San Jose, CA, USA).

Reverse transcription quantitative polymerase chain reaction (RT-qPCR)

Total RNA in the tissues and cultured cells was extracted by TRIzol (Thermo Fisher Scientific, MA, USA) as per the manufacturer's requirements. Next, the reverse transcription of RNA into cDNA was realized by Reverse Transcription System (Promega, WI, USA). The expression levels of target genes were tested by a LightCycler 480 fluorescence quantitative PCR instrument (Roche, IN, USA). The reaction conditions were carried out based upon the instructions of the fluorescent quantitative PCR kit (SYBR Green PCR kit, Takara Bio, Inc., Otsu, Japan): 95 °C pre-denaturation for 5 min, and next, with 40 cycles of 95 °C denaturation for 10 s, 60 °C annealing for 10 s and 72 °C extension for 20 s. Glyceraldehyde phosphate dehydrogenase (GAPDH) and U6 were selected as the standardized controls. Data were analyzed using $2^{-\Delta\Delta Ct}$ method and the primer sequences were shown in **Table 1**.

Table 1
Primer sequence.

Name	Primer sequence
miR-301a-3p	F: 5′-ACACTCCAGCTGGGCAGTGCAATAGTATTGTC-3′
	R: 5′- CTCAACTGGTGTCGTGGA-3′
U6	F: 5′-CTCGCTTCGGCAGCACA-3′
	R: 5′-AACGCTTCACGAATTTGCGT-3′
RBPMS-AS1	F: 5′-GAGAAGGAGAACACCCCGAG-3′
	R: 5′-TGGAGTTACGCAATTTGGGG-3′
NRGN	F: 5′- CCAGGAGCTCACCTGTTTCT-3′
	R: 5′- CTTTTCTCCCACTCACGGGT-3′
CAMTA1	F: 5′-ATCCTTATCCAGAGCAAATTCC-3′
	R: 5′- AGTTTCTGTTGTACAATCACAG-3′
GAPDH	F: 5′-GTCAGTGGTGGACCTGACCT-3′
	R: 5′- TGCTGTAGCCAAATTCGTTG-3′

Note: miR, microRNA; CAMTA1, calmodulin-binding transcription activator 1; NRGN, neurogranin; GAPDH, glyceraldehyde phosphate dehydrogenase; F, forward; R, reverse.

Western blot analysis

The extraction of proteins were from cells and tissues of each group and the protein concentration was measured with the application of the bicinchoninic acid protein kit. After that, the protein samples were separated on 10% sodium dodecyl sulfate-polyacrylamide gel electrophoresis gel, transferred onto membranes (300 mA) and blocked by 5% skimmed milk powder for 1 hour. Next, the membranes were incubated with primary antibody against CAMTA1 (ab227713, 1:1000, Abcam, Cambridge, MA, USA) and neurogranin (NRGN, ab217672, 1:1000, Abcam) (overnight, 4℃). Subsequently, the cells were incubated with horseradish peroxidase-conjugated secondary antibody (Abcam) at 37℃ for 1 h. The bands were visualized with chemiluminescent reagents. The signal intensities of the proteins were evaluated using Image J software.

Dual luciferase reporter gene assay

According to the Starbase v3.0 database (http://starbase.sysu.edu.cn/), the miRNAs that bound to RBPMS-AS1 and CAMTA1 were predicted, and the sequences of RBPMS-AS1-wild type (WT) and RBPMS-AS1-mutant type (Mut), together with CAMTA1-WT and CAMTA1-Mut, containing the binding site were separately designed and synthesized based upon the results of the prediction. The Wt sequence and Mut sequence containing the binding site were respectively inserted into the luciferase reporter vector (PGL3-Promoter or PGL3-Basic) to obtain a reporter plasmid. The 293T cells (2.5×10^5 cells) were seeded onto a 24-well culture dish. The next day, the reporter cells and effectors were transfected into cells with FuGENE HD Transfection Reagent (Roche Applied Science) based upon the manufacturer's instructions. Simultaneously, the miR-301a-3p mimic or mimic-NC was transfected into the cells. After 48-hour transfection, the cells were collected, lysed and centrifuged for 3 to 5 min to obtain the supernatant, and the luciferase activity in the cell extract was analyzed using a Luciferase Assay Kit (Dual-Luciferase Reporter Assay System, Promega). The value of the target luciferase/luciferase of the internal control was used as a relative luciferase activity, and the luciferase value was measured with a fluorescent detector (Promega). Three parallel experiments were performed.

Plasmids

A CAMTA1-WT plasmid or a mutant lacking DNA binding domain (CAMTA1-Mut) was constructed according to a reference [24]. After the plasmid was transfected into U251 and U87 cells, NRGN expression level was detected by RT-qPCR.

RNA pull-down assay

The biotinylated miR-301a-3p-WT or miR-301a-3p-Mut or negative control (NC) were utilized for the treatment of U251 and U87 cells. Then streptavidin-coated magnetic beads (Ambion, Austin, TX, USA) were supplemented in the cell lysate. The enrichment of RBPMS-AS1 and CAMTA1 was conducted by RT-qPCR with the pull down of the biotin-coupled RNA complex.

Animal

Twenty-four specific pathogen-free grade (SPF) BALB/c nude mice (4–6 weeks old, 16–20 g, male) from Beijing Vital River Laboratory Animal Technology Co., Ltd. (Beijing, China) were randomly selected into our experiment. The padding, drinking water, particulate feed, and other articles in contact with the animal were treated with autoclaved sterilization. All experimental animals were raised in a SPF-level aseptic layer under the conditions of a constant temperature of (22–26 °C) and a constant humidity of (55 ± 5%).

An orthotopic xenograft model in nude mice

U251 cells were infected with a lentivirus containing a Luciferase and a green fluorescent protein (GFP), and the flow cytometry was utilized to screen the stably-expressing GFP-Luc cell lines. The nude mice were randomly assigned into a Vector group (transfection of pcDNA3.1 in U251-GFP-Luc cell suspension) and a pcDNA3.1-RBPMS-AS1 group (transfection of pcDNA3.1-RBPMS-AS1 in U251-GFP-Luc cell suspension). Upon 24-hour transfection of U251-GFP-Luc cells, the nude mice were anesthetized by intraperitoneal injection with pentobarbital sodium (60 mg/kg). After anesthesia, the head skin of the nude mice was disinfected by conventional iodophor, and then the nude mice were fixed in the middle of the triangle with a stereotactic instrument. The head skin was cut vertically along 3 mm to the right of the longitudinal midline of the head and at the junction with the two ears to expose the skull. The skull of the nude mouse was opened using a dental drill at 2 mm to the right of the bilateral eye and ear junction. The transfected or untransfected U251-GFP-Luc cell suspension (3×10^5) was absorbed using a sterilized microsample sampler. The needle was inserted along the bore for approximately 3 mm, and then backed for 1 mm, and the rats were slowly injected with 100 μL cell suspension. After injection, the boreholes were closed with bone wax, the skin incision was stitched, the wound was disinfected, and the nude mice were placed back to the cage for feeding after recovery from anesthesia.

Nude mouse irradiation

After the orthotopic xenograft model was successfully established, the nude mice with two groups (Vector group and pcDNA3.1-RBPMS-AS1 group) determined by live imaging scan were randomly divided into radiotherapy and non-radiotherapy groups, namely all orthotopic xenograft models into four groups: non-radiotherapy or radiotherapy RBPMS-AS1 group (RBPMS-AS1-IR or RBPMS-AS1-non-IR group) and non-radiotherapy or radiotherapy Vector group (Vector-IR or Vector-non-IR group). Whole cranial irradiation of nude mice was performed 3 times at a bolus dose of 2 Gy each time, for a total of 6 Gy, and the irradiation was completed within a week. The live imaging of nude mice was performed again after radiotherapy.

Live imaging scan

After 21 days and 42 days, the nude mice were intraperitoneally injected with luciferase substrate (substrate concentration: 15 mg/mL, 10 μL/g), and the change of luminescence signal was observed on a small animal Live Imager (IVIS Spectrum, Caliper, USA) to analyze the brain tumorigenesis and growth status. Nude mice were subsequently anesthetized and euthanized, and the skull was dissected to preserve the tissues for reserve.

Immunohistochemistry

Tumor tissue samples for in vivo experiments were first fixed with 4% paraformaldehyde, and then embedded and cut with paraffin. Continuous 4-μm thick sections were selected for immunohistochemical analysis using anti-Ki67 antibody (Santa Cruz Biotechnology, Dallas, TX).

Statistical analysis

Unless otherwise stated, all experiments were repeated three times. All data analyses were conducted using SPSS 18.0 software (IBM Corp. Armonk, NY, USA) and GraphPad Prism 6.0 (GraphPad Software Inc.). Data were reported as mean ± standard deviation. The *t*-test was performed for comparisons between two groups, and one-way analysis of variance (ANOVA) was conducted for comparisons among multiple groups and Tukey's multiple comparisons test was used for pairwise comparisons after one-way ANOVA. *p* value less than 0.05 was indicative of statistically significant difference.

Results

RBPMS-AS1 enhances the radiosensitivity of GBM

The copy number variation of RBPMS-AS1 is positively related to the overall survival of lung adenocarcinoma patients [12], while it has not been studied in GBM. In our research, we performed RT-qPCR to detect the RBPMS-AS1 expression level in GBM tissues and the corresponding normal tissues, and the results of which showed that decreased RBPMS-AS1 expression was observed in GBM tissues in comparison to normal tissues (Fig. 1A). In addition, GBM cells (A172, LN229, U251 and U87) also had lower expression levels of RBPMS-AS1 than NHA cells, while the RBPMS-AS1 expression level in U251 and U87 cells was relatively lower, thus we selected U251 and U87 cells for the subsequent experiments (Fig. 1B).

Additionally, RBPMS-AS1 expression level was detected in U251 and U87 cells post exposure to varying doses of irradiation. Similarly, in U251 and U87 cells, RBPMS-AS1 expression level decreased with increasing dose of irradiation treatment (Fig. 1C), and the reduction of RBPMS-AS1 expression was more significant with the irradiation dose of 6 Gy and 8 Gy. These data indicate that RBPMS-AS1 may be related to the radiosensitivity of GBM.

For the purpose of exploring the effect of RBPMS-AS1 on the

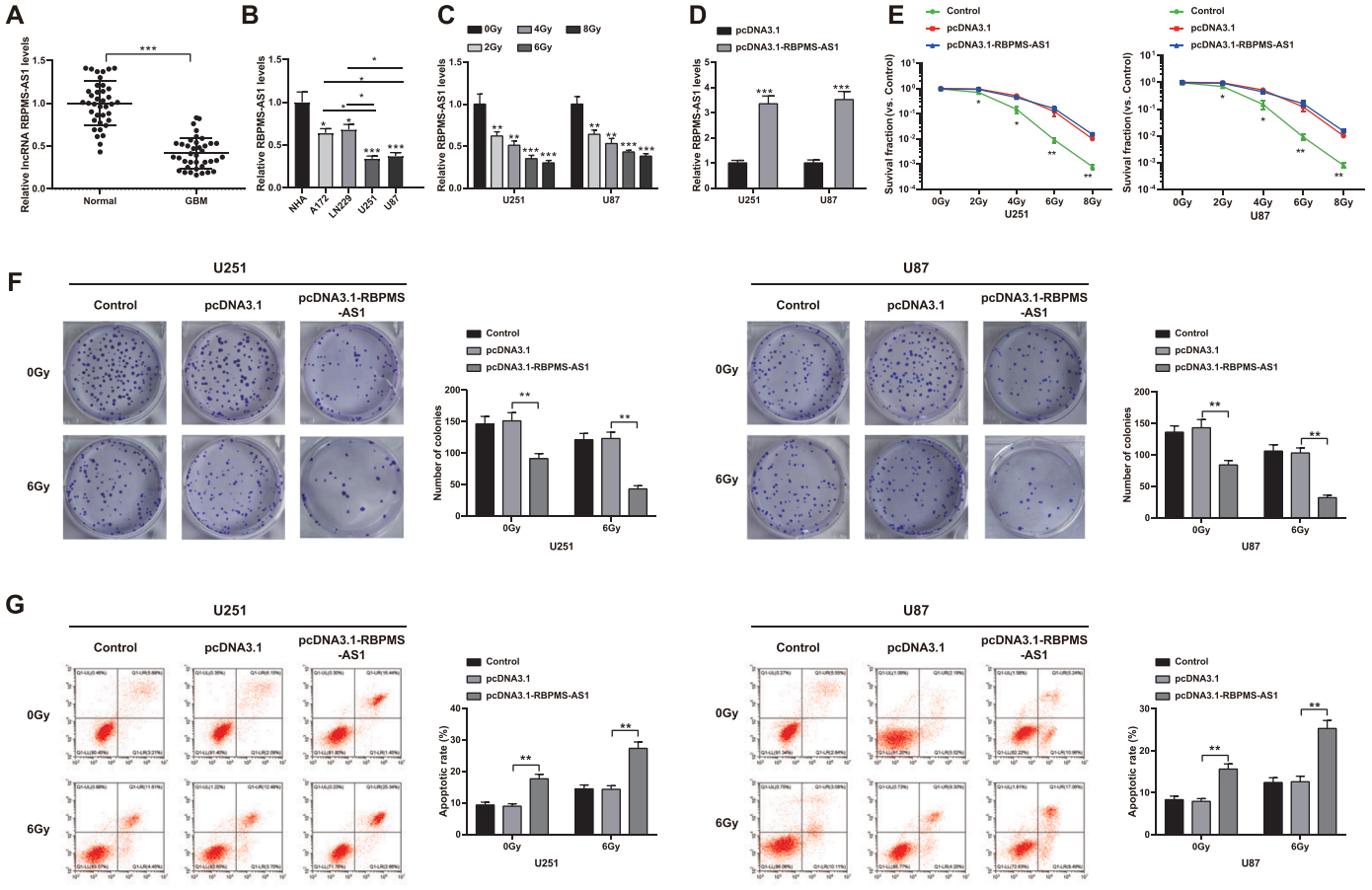

Fig. 1. RBPMS-AS1 promotes radiosensitivity of GBM.
A. RT-qPCR was conducted to detect the RBPMS-AS1 RNA expression level in GBM tissues and normal tissues. B. RT-qPCR was performed to detect the expression level of RBPMS-AS1 in NHA cells and GBM cells (A172, LN229, U251 and U87). C. RT-qPCR was implemented to detect RBPMS-AS1 expression level in U251 and U87 cells under different doses (2, 4, 6 and 8 Gy) of X-ray irradiation. D. RT-qPCR was utilized to detect the RBPMS-AS1 expression level in U251 and U87 cells upon transfection of pcDNA3.1-RBPMS-AS1. E. MTT assay was utilized to evaluate the survival of U251 and U87 cells (overexpressing or not overexpressing RBPMS-AS1) under 0, 2, 4, 6 and 8 Gy X-ray irradiation. F. Colony formation assay was conducted to detect the proliferation of transfected cells at 0 and 6 Gy X-ray irradiation. G. Flow cytometry was performed to detect apoptosis of transfected cells under 0 and 6 Gy X-ray irradiation. In panel A, $n = 38$; in panel B-G, $N = 3$. *, $p < 0.05$, **, $p < 0.01$; ***, $p < 0.001$. The *t*-test was performed for comparisons between two groups, one-way ANOVA was utilized for comparisons among multiple groups and Tukey's multiple comparisons test was used for pairwise comparisons after one-way ANOVA.

radiosensitivity of GBM, we transfected pcDNA3.1-RBPMS-AS1 into U251 and U87 cells, and the RT-qPCR method verified the successful transfection (Fig. 1D). According to the findings of MTT assay, we found that RBPMS-AS1 overexpression enhanced the radiosensitivity of U251 and U87 cells (Fig. 1E). In addition, the results of colony formation assay and flow cytometry indicated that when RBPMS-AS1 was overexpressed, the inhibition of cell proliferation resulted from the increased radiation dose was further enhanced (Fig. 1F), and the apoptosis caused by the increase in radiation dose was also further enhanced (Fig. 1G). Therefore, we conclude that RBPMS-AS1 promotes radiosensitivity of GBM.

Upregulation of CAMTA1 enhances radiosensitivity of GBM

The Genecards website shows that CAMTA1 contains a transcription factor immunoglobulin domain, ankyrin repeats, as well as calmodulin-binding IQ motifs. CAMTA1 acts as a tumor inhititory gene in gliomas [21], and there is a report revealing that CAMTA1 is acted as a transcription factor to activate the transcription of cardiac hormone sodium A (NPPA), and induces anti-proliferation effects in glioma cells [24]. In our research, we performed RT-qPCR to detect the CAMTA1 expression level in GBM tissues and the corresponding normal tissues, which revealed that decreased CAMTA1 expression was found in GBM tissues versus normal tissues (Fig. 2A). In addition, GBM cells (A172, LN229, U251 and U87) also exhibited lower expression levels of CAMTA1 than

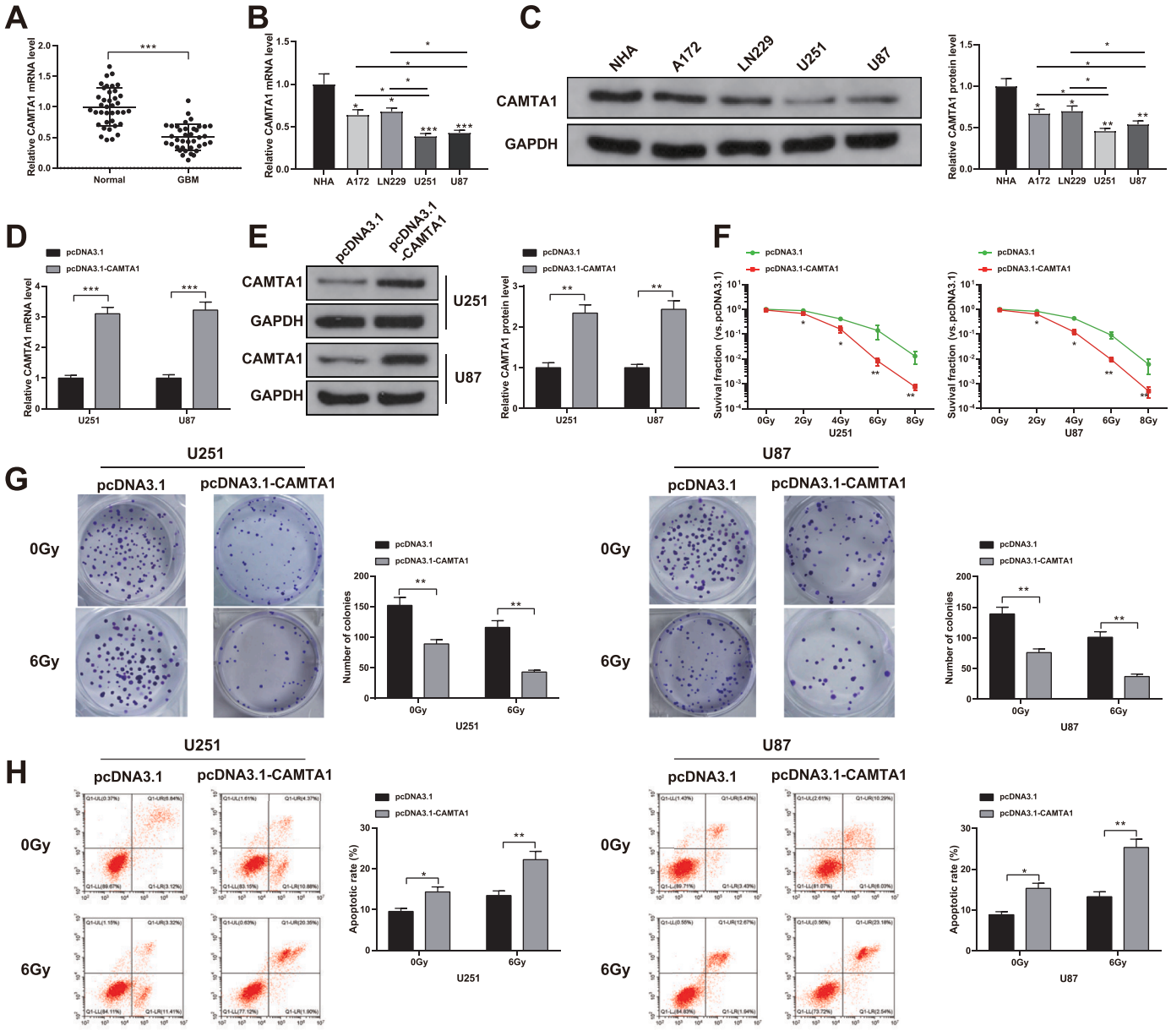

Fig. 2. CAMTA1 induces radiosensitivity of GBM.
A. RT-qPCR was conducted to detect the expression level of CAMTA1 in GBM tissues and normal tissues. B-C. RT-qPCR and Western blot assays were implemented to detect the CAMTA1 expression level in NHA cells and GBM cells (A172, LN229, U251 and U87). D-E. RT-qPCR and Western blot assay were adopted to detect CAMTA1 expression level in U251 and U87 cells upon transfection of pcDNA3.1-CAMTA1. F. MTT assay was utilized to evaluate the survival of U251 and U87 cells (overexpressing or not overexpressing CAMTA1) under 0, 2, 4, 6 and 8 Gy X-ray irradiation. G. Colony formation assay was conducted to detect the proliferation of transfected cells at 0 and 6 Gy X-ray irradiation. H. Flow cytometry was performed to detect apoptosis of transfected cells under 0 and 6 Gy X-ray irradiation. In panel A, $n = 38$; in panel B-H, $N = 3$. *, $p < 0.05$, **, $p < 0.01$; ***, $p < 0.001$. The *t*-test was performed for comparisons between two groups, one-way ANOVA was used for comparisons among multiple groups and Tukey's multiple comparisons test was used for pairwise comparisons after one-way ANOVA.

NHA cells based on the results of RT-qPCR and Western blot assays (Fig. 2B,C). Subsequently, we transfected pcDNA3.1-CAMTA1 into U251 and U87 cells, and the RT-qPCR and Western blot assay verified the successful transfection (Fig. 2D,E). From the findings of MTT assay, colony formation assay and flow cytometry, we could see that CAMTA1 overexpression enhanced the radiosensitivity of U251 and U87 cells (Fig. 2F), promoted the suppression of cell proliferation and also the apoptosis caused by the increased radiation dose (Fig. 2G,H). These findings indicate that CAMTA1 enhances the radiosensitivity of GBM.

RBPMS-AS1 enhances the expression of CAMTA1 in GBM cells through sponging miR-301a-3p

Recently, emerging studies have reported the role of lncRNA in the competitive endogenous RNA (ceRNA) network. Therefore, whether there was a relationship between RBPMS-AS1 and CAMTA1 raised our interest. Based on this, we speculated that RBPMS-AS1 may affect CAMTA1 expression in GBM cells through the ceRNA mechanism. Furthermore, whether there was a relationship between RBPMS-AS1 and CAMTA1 in GBM intrigued us. We observed that overexpressed RBPMS-AS1 could stimulate the CAMTA1 expression in U251 and U87 cells (Fig. 3A,B). This indicates that RBPMS-AS1 regulates the expression of CAMTA1 in GBC cells.

According to the prediction of starBase v3.0, 17 miRNAs were found to simultaneously bind to RBPMS-AS1 and CAMTA1 (Fig. 3C). Among these 17 miRNAs, only miR-34c-5p, miR-4295, miR-301a-3p, and miR-301b-3p were up-regulated in GBM cells, and miR-301a-3p was up-regulated most significantly (Fig. 3D). Therefore, we selected miR-301a-3p for the follow-up experiments.

Subsequently, we investigated whether miR-301a-3p was involved in the mechanism of ceRNA. First, we used a bioinformatics tool to predict the binding sequence of miR-301a-3p and RBPMS-AS1 or miR-301a-3p and CAMTA1 (Fig. 3E). Through a dual luciferase reporter assay, it was verified that relative to the control, the luciferase activity of cells inserted with RBPMS-AS1-WT or CAMTA1-WT was significantly reduced when miR-301a-3p was overexpressed, while the luciferase activity of RBPMS-AS1-Mut or CAMTA1-Mut was not affected by miR-301a-3p mimic (Fig. 3F). Importantly, RNA pull-down assay (Fig. 3G) suggested that versus the control, both RBPMS-AS1 and CAMTA1 enrichment was elevated in U251 and U87 cells introduced with biotinylated miR-301a-3p-WT, while the cells introduced with biotinylated miR-301a-3p-Mut failed to enrich RBPMS-AS1 and CAMTA1, suggesting the interaction of miR-301a-3p with RBPMS-AS1 and CAMTA1. Additionally, in cells with miR-301a-3p mimic treatment, CAMTA1

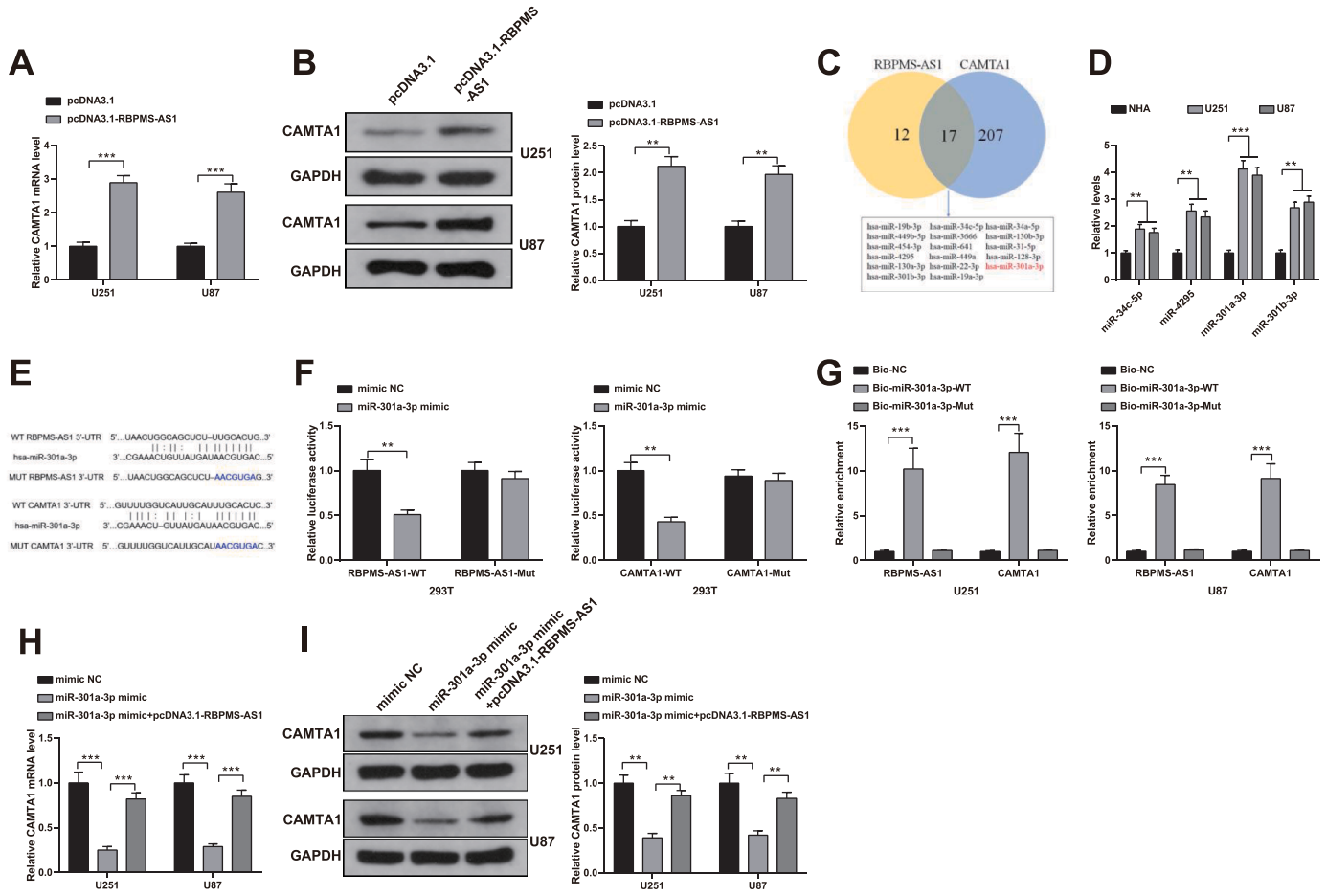

Fig. 3. RBPMS-AS1 increases the expression of CAMTA1 in GBM cells through sponging miR-301a-3p.
A-B. RT-qPCR and Western blot assay were conducted to detect the mRNA and protein levels of CAMTA1 in U251 and U87 cells overexpressing RBPMS-AS1. C. starBase v3.0 predicted that 17 miRNAs were found to simultaneously bind to RBPMS-AS1 and CAMTA1. D. RT-qPCR was carried out to detectmiR-34c-5p, miR-4295, miR-301a-3p, and miR-301b-3p expression levels in NHA cells and GBM cells (U251 and U87). E. starBase v3.0 predicted the binding sequence of miR-301a-3p and RBPMS-AS1 or miR-301a-3p and CAMTA1. F. Dual luciferase reporter gene assay was conducted to verify the target relationship between miR-301a-3p and RBPMS-AS1 or miR-301a-3p and CAMTA1. G. RNA pull-down assay was utilized to detect the interaction between miR-301a-3p and RBPMS-AS1 or miR-301a-3p and CAMTA1. H-I. RT-qPCR and Western blot assay were conducted to detect the mRNA and protein levels of CAMTA1 in GBM cells of each group. $N = 3$. **, $p < 0.01$; ***, $p < 0.001$. The *t*-test was performed for comparisons between two groups, one-way ANOVA was used for comparisons among multiple groups and Tukey's multiple comparisons test was used for pairwise comparisons after one-way ANOVA.

expression levels were decreased, which was subsequently restored by upregulation of RBPMS-AS1 (Fig. 3H,I). These data imply that RBPMS-AS1 increases the expression of CAMTA1 in GBM cells through sponging miR-301a-3p.

RBPMS-AS1 inhibits GBM cell proliferation and radiotherapy resistance through miR-301a-3p/CAMTA1 axis

For further exploring whether RBPMS-AS1 inhibited GBM cell proliferation and radiotherapy resistance through the miR-301a-3p/CAMTA1 axis, we transfected mimic NC, miR-301a-3p mimic, or miR-301a-3p mimic + pcDNA3.1-RBPMS-AS1/pcDNA3.1-CAMTA1 simultaneously in U251 and U87 cells, respectively. The results of RT-qPCR and Western blot assay indicated that elevated expression level of miR-301a-3p and reduced RBPMS-AS1 and CAMTA1 expression levels were found in GBM cells upon miR-301a-3p mimic treatment, while the effects of miR-301a-3p mimic on the miR-301a-3p, RBPMS-AS1 and CAMTA1 expression levels were counteracted in GBM cells in response to further transfection with pcDNA3.1-RBPMS-AS1; however, the expression level of CAMTA1 increased significantly, while the expression levels of RBPMS-AS1 and miR-301a-3p did not change in GBM cells further transfected with pcDNA3.1-CAMTA1 (Fig. 4A,B). Meanwhile, the functional experiments suggested that restoration of miR-301a-3p diminished the radiosensitivity of U251 and U87 cells (Fig. 4C), weakened the restriction of cell proliferation and also weakened the apoptosis caused by the increased radiation dose (Fig. 4D,E). However, GBM cells exposed to radiation showed promoted radiosensitivity, reduced proliferation, and enahnced apoptosis when RBPMS-AS1 or CAMTA1 was upregulated despite overexpressed miR-301a-3p (Fig. 4C-E). The above results reveal that RBPMS-AS1 restricts GBM cell proliferation and radiotherapy resistance through the miR-301a-3p/CAMTA1 axis.

CAMTA1 promotes NRGN expression

The JASPAR database shows that CAMTA1 can be used as a transcription factor to bind to the promoter region of the downstream gene NRGN to regulate NRGN expression (Fig. 5A). Interestingly, an *in-vitro* experiment has suggested that NRGN has an anti-proliferative effect on GBM cells [26]. We, therefore, analyzed whether CAMTA1 also activated the expression of NRGN in GBM cells.

U251 and U87 cells were treated with a plasmid expressing CAMTA1-WT or a mutant lacking a DNA binding domain, in which NRGN expression was analyzed by RT-qPCR (Fig. 5B). There was an increased NRGN expression level in cells transfected with CAMTA1-WT plasmid, while the NRGN expression in cells transfected with CAMTA1-Mut plasmid was slightly increased, compared with cell transfection with empty plasmid.

Furthermore, because RBPMS-AS1 and miR-301a-3p could regulate CAMTA1 expression in GBM cells, we tested NRGN expression in cells upon transfection of pcDNA3.1-RBPMS-AS1 or the simultaneous

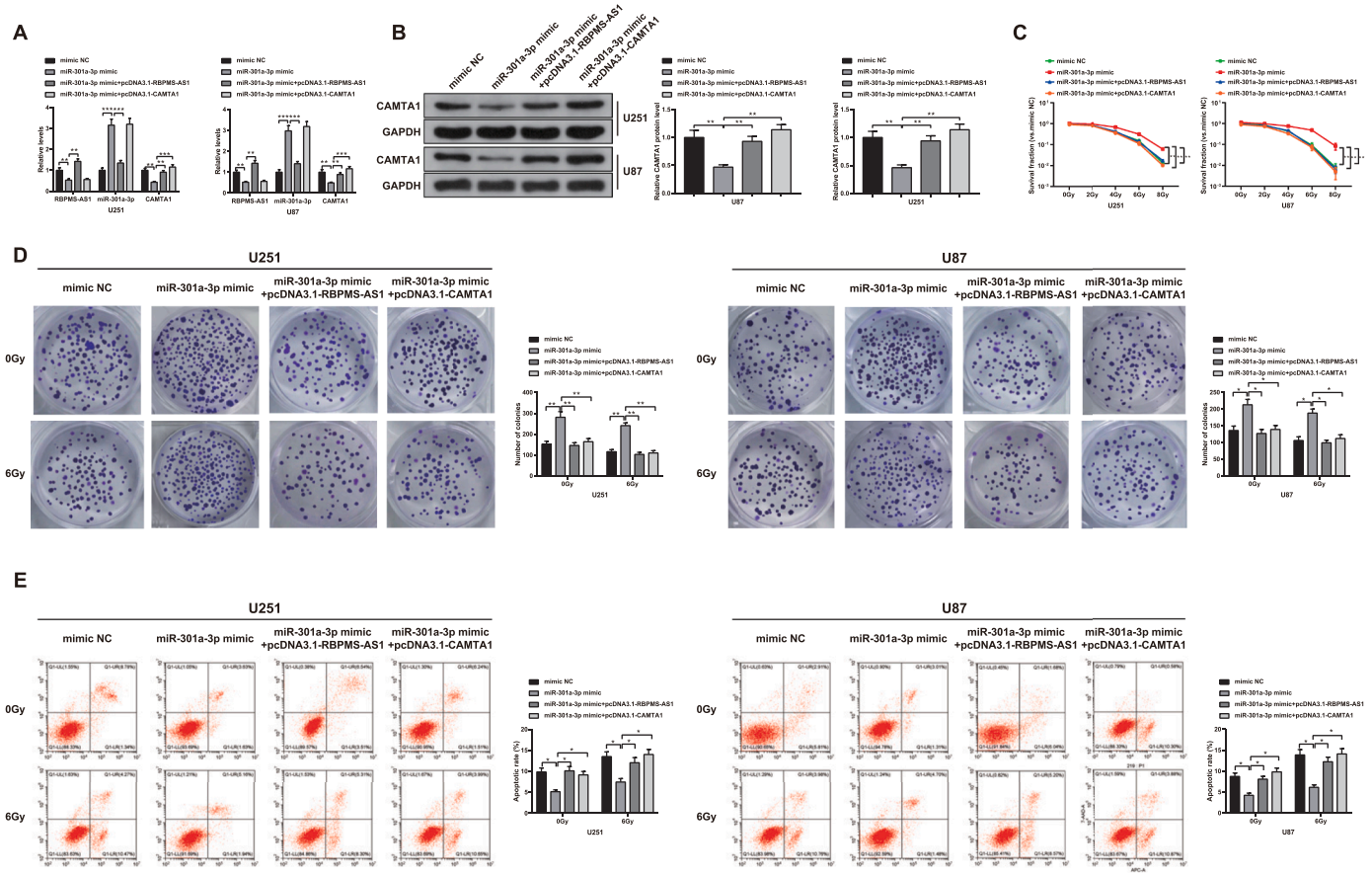

Fig. 4. RBPMS-AS1 restricts GBM cell proliferation and radiotherapy resistance through the miR-301a-3p/CAMTA1 axis.
A. RBPMS-AS1, miR-301a-3p and CAMTA1 expression levels in transfected U251 and U87 cells in each group were tested by RT-qPCR. B. CAMTA1 expression level in transfected U251 and U87 cells in each group were tested by Western blot assay. C. The survival conditions of transfected U251 and U87 cells in each group under 0, 2, 4, 6 and 8 Gy X-ray irradiation were measured by MTT assay. D. The proliferation conditions of transfected U251 and U87 cells in each group at 0 and 6 Gy X-ray irradiation were detected by colony formation assay. E. The apoptosis rates of transfected U251 and U87 cells in each group at 0 and 6 Gy X-ray irradiation were tested by flow cytometry. $N = 3$. *, $p < 0.05$, **, $p < 0.01$; ***, $p < 0.001$. One-way ANOVA was used for comparisons among multiple groups and Tukey's multiple comparisons test was used for pairwise comparisons after one-way ANOVA.

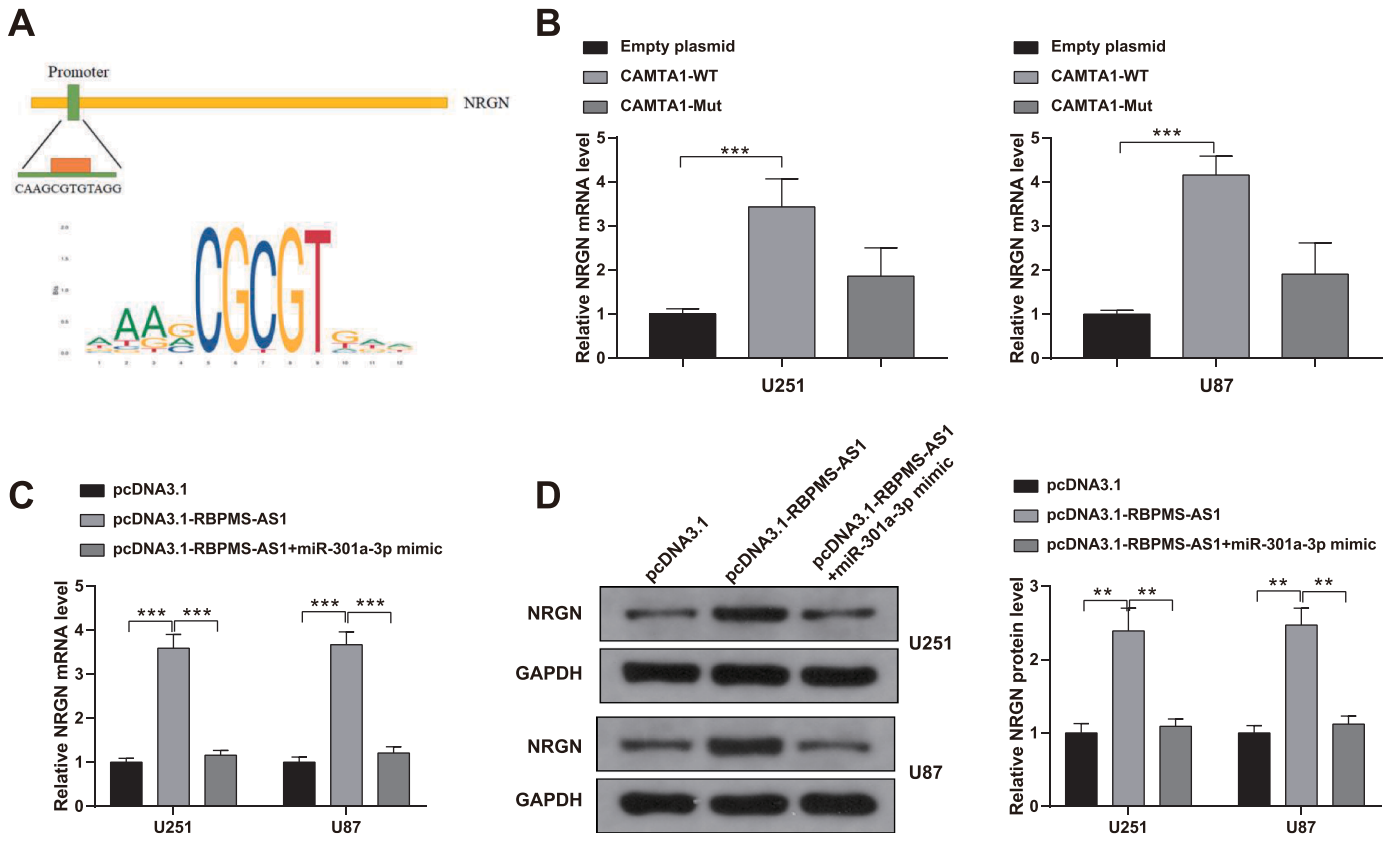

Fig. 5. CAMTA1 axis promotes NRGN transcription.
A. The binding base sequence of CAMTA1 and NRGN promoter region. B. RT-qPCR analysis of NRGN expression in U251 and U87 cells treated with plasmids expressing CAMTA1-WT or mutants lacking DNA binding domains. C-D. RT-qPCR and Western blot assay were adopted to detect NRGN expression in GBM cells upon transfection of pcDNA3.1-RBPMS-AS1 or the simultaneous transfection of pcDNA3.1-RBPMS-AS1 and miR-301a-3p mimic. $N = 3$. **, $p < 0.01$; ***, $p < 0.001$. One-way ANOVA was used for comparisons among multiple groups and Tukey's multiple comparisons test was used for pairwise comparisons after one-way ANOVA.

transfection of pcDNA3.1-RBPMS-AS1 and miR-301a-3p mimic. It was found that there was an elevation in NRGN expression in GBM cells upon transfection of pcDNA3.1-RBPMS-AS1, while the expression of which was reversed in GBM cells upon the simultaneous transfection of pcDNA3.1-RBPMS-AS1 and miR-301a-3p mimic (Fig. 5C,D). The above results imply that NRGN expression in GBM cells may be achieved through this regulatory network of the RBPMS-AS1/miR-301a-3p/CAMTA1 axis.

RBPMS-AS1 inhibits the formation and radiosensitivity of in situ tumors in vivo

With the aim to further clarify the anti-tumor effect of RBPMS-AS1 in vivo, we conducted an orthotopic xenograft model and radiotherapy experiment in nude mice. pCDNA3.1 or pCDNA3.1-RBPMS-AS1 was transfected in U251 cells, and the cell suspension was prepared upon 24-hour transfection, which was then transplanted into nude mice. Live imaging results in nude mice showed that the fluorescence intensity in the Vector-non-IR group was significantly stronger than that in the RBPMS-AS1-non-IR group; the fluorescence intensity was further decreased in the Vector-IR group compared to the Vector-non-IR group; and the fluorescence intensity was further decreased in the RBPMS-AS1-IR group compared to the RBPMS-AS1-non-IR group (Fig. 6A). The results of immunohistochemistry indicated that before radiotherapy, RBPMS-AS1 overexpression inhibited the positive expression of Ki67, and RBPMS-AS1 overexpression further inhibited the positive expression of Ki67 after radiotherapy (Fig. 6B). The above results indicated that RBPMS-AS1 overexpression inhibited the transplanted tumor growth of U251 cells in nude mice and further inhibited the growth of transplanted tumors in nude mice after receiving the same dose of radiotherapy. The findings of this research suggest that RBPMS-AS1 overexpression may be related to the greater sensitivity of U251 cells to radiotherapy in animals.

Discussion

GBM is difficult to treat for involving the genetic and chromosomal aberrations, which causes tumor cells invade aggressively and proliferate uncontrollably [3]. Standard treatments include surgical resection, external beam radiation, and chemotherapy containing varied inhibitors, while no known curative therapy has been found [27, 28]. Hence, it is crucial to explore more effective therapeutic agents that can prevent the growth of GBM cells and the mechanisms underlying the acquirement of radiosensitivity in GBM.

A growing number of articles have illustrated that dysregulated lncRNAs are able to participate in diverse tumors, including glioma [29, 30]. For instance, Liu et al. have found that lncRNA OIP5-AS1 controls the biological processes in glioma via mediating microRNA (miR)–367–3p/CEBPA [31]. Zheng et al. have stated that lncRNA CRNDE induces glioma progression via modulating miR-384/PIWIL4/STAT3 signaling [32]. In our research, we detected the expression level of RBPMS-AS1 in GBM tissues and cells, and the results presented decreased expression level of RBPMS-AS1. In addition, the results of functional experiments indicated that upregulated RBPMS-AS1 promoted the radiosensitivity of GBM cells. Similarly, Wang et al. have found that RBPMS-AS1 is lowly expressed in LUAD tissues verus normal tissues, and low expression of RBPMS-AS1 is related to poorer overall survival of LUAD patients [12]. Nevertheless, the role of RBPMS-AS1 in

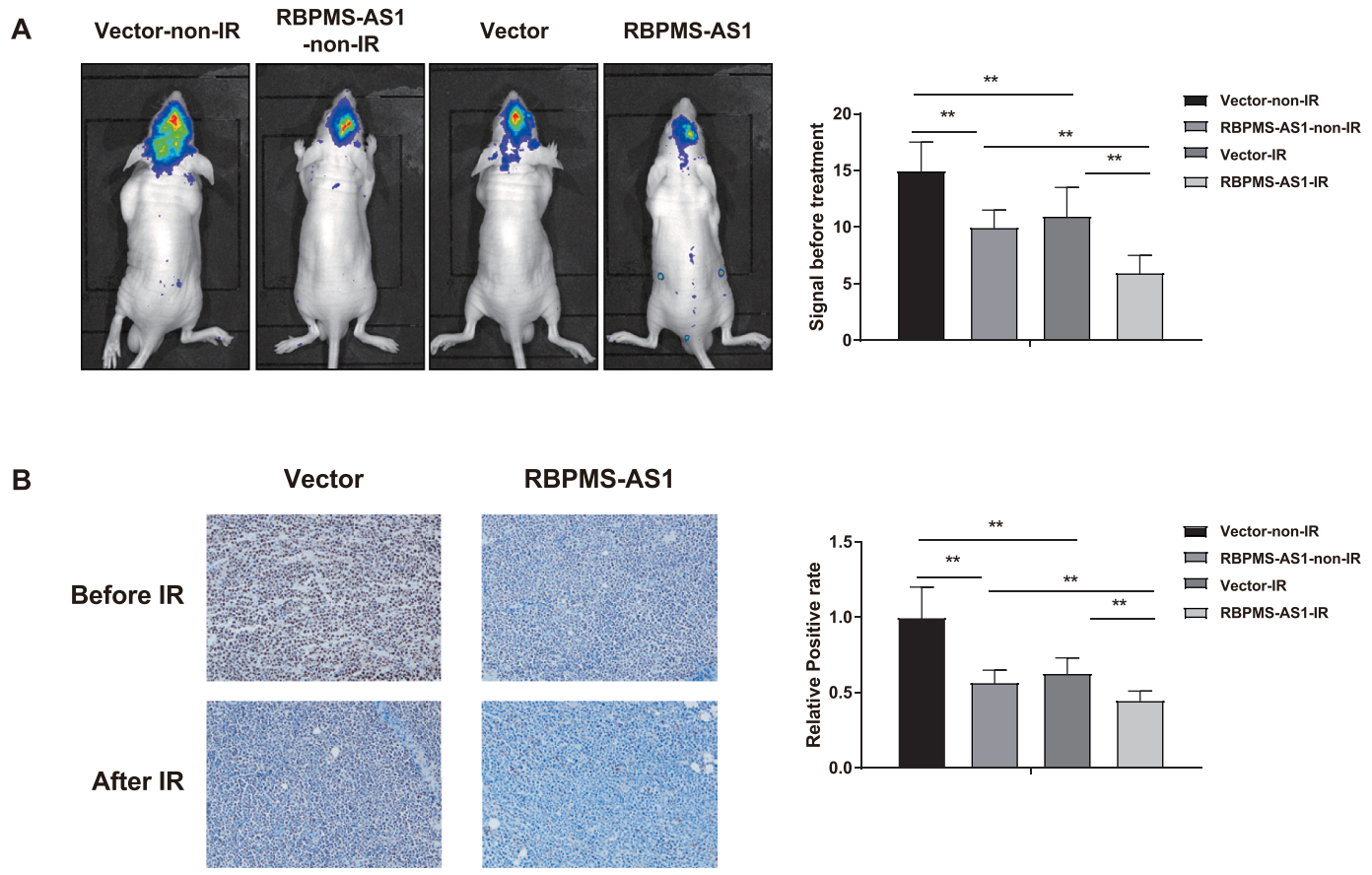

Fig. 6. RBPMS-AS1 inhibits the formation and radiosensitivity of in situ tumors in vivo.
A. Live imaging of transplanted tumors in nude mice in each group. B. Immunohistochemical detection of Ki67 protein expression in tumor tissues of nude mice in each group. $n = 6$. **, $p < 0.01$. One-way ANOVA was used for comparisons among multiple groups and Tukey's multiple comparisons test was used for pairwise comparisons after one-way ANOVA. The Vector and RBPMS-AS1 groups were the U251-GFP-Luc cell suspension transfected with pcDNA3.1 and pcDNA3.1-RBPMS-AS1.

the radiosensitivity of GBM and its mechanism need further confirmation.

In our study, it was found that overexpressed RBPMS-AS1 could stimulate the CAMTA1 expression level in U251 and U87 cells, implying that the association of CAMTA1 and RBPMS-AS1 in GBM cells. CAMTA1 is of great importance in diverse human cancers, acting as a tumor inhibitive gene in neuroblastomas, gliomas and colorectal cancers [23, 33, 34]. In accord with RBPMS-AS1, CAMTA1 was also proposed a regulatory factor of radiosensitivity in GBM in our research. In a prior research, CAMTA1 overexpression has been found to suppress cell colony formation and growth rate, and also restrict in vivo growth in nude mice, strengthening the role of CAMTA1 as a tumor inhibitor candidate [35]. Strikingly, CAMTA1 has been implied to have an anti-tumor activity in neuroblastoma cells, which functions the same in many neural tumors [35]. Furthermore, CAMTA1 leads to a strong diminish of colony formation, implying that CAMTA1 is an anti-tumor factor in GBM [24].

Subsequently, we eludicated whether miR-301a-3p was involved in ceRNA mechanism, and the data implied that RBPMS-AS1 increased CAMTA1 expression in GBM cells through sponging miR-301a-3p. Meanwhile, the functional experiments suggested that upregulation of miR-301a-3p diminished the radiosensitivity and apoptosis, and increased proliferation of GBM cells. However, the functions of upregulated miR-301a-3p on the malignant features of GBM cells were counteracted by upregulation of RBPMS-AS1 and CAMTA1, revealing that RBPMS-AS1 restricted GBM cell proliferation and radiotherapy resistance through the miR-301a-3p/CAMTA1 axis. Numerous studies have suggested that miR-301a-3p could induce the malignant phenotypes of cancer cells. The findings in Xia et al. have confirmed that the restoration of miR-301a-3p can stimulate the gemcitabine cytotoxicity towards human pancreatic ductal adenocarcinoma cells [36]. Another study has demonstrated that miR-301a-3p is increased in patients with treatment resistance, and reduced in patients responsive to the treatment, supporting that miR-301a-3p is an indicator in epileptic patients to determine treatment resistance [37]. In line with our findings, the reduced miR-301a-3p expression in tumor tissues are capable of identifying a subgroup of GBM patients that had been treated with regorafenib with profitable benefit [19].

Moreover, the JASPAR database predicted that CAMTA1 could be used as a transcription factor to bind to the promoter region of the downstream gene NRGN to regulate NRGN expression. Recently, the significance of NRGN has been recognized in several brain-related diseases, including schizophrenia, Parkinson's disease and Alzheimer disease [38–40]. Previously, Yokota et al. have reported that NRGN is downregulated in GBM tissues [25]. Also, an *in-vitro* experiment has disclosed that NRGN has an anti-proliferative effect on GBM cells [26]. In the present article, we also implied that RBPMS-AS1 and miR-301a-3p might regulate the NRGN expression in GBM cells through modulating CAMTA1.

In previous researches, YAP and TAZ are two proteins often associated with the CAMTA1 function [41, 42]. The Hippo pathway transcriptional coactivators YAP/TAZ have been considered as drivers in GBM progression, which could be used as therapeutic targets [43]. Evidence has shown that YAP and TAZ are upregulated in epidermal growth factor receptor (EGFR)-amplified/mutant human GBMs, and the downregulation of YAP and TAZ inhibit proliferation and elicit apoptosis in EGFR-amplified/mutant GBM cells [44]. Lei Zhang et al.

have stated that depletion of TAZ induces radiation-induced growth arrest, and the β-catenin destruction complex activation could promote radiation-induced TAZ suppression and growth arrest in GBM tumor cells [45]. Due to time and funding issues, we failed to explore the regulatory mechanisms of RBPMS-AS1, CAMTA1, and YAP and TAZ in GBM, which would be the research point in our further study. Additionally, the regulation of radiosensitivity in GBM by the RBPMS-AS1/miR-301a-3p/CAMTA1 axis necessitates more extensive animal experiments.

Together, our data suggest that RBPMS-AS1 promotes NRGN transcription through the miR-301a-3p/CAMTA1 axis and enhances the radiosensitivity of GBM. Understanding the function of RBPMS-AS1 may help unearth effective therapeutic strategies for GBM patients. Further dissection of RBPMS-AS1 downstream signaling and understanding of mechanisms modulating RBPMS-AS1 will be the next research focal point.

Authors' contribution

JYG and LWY conceived the ideas. JYG and LWY designed the experiments. LWY and C. Yan performed the experiments. LWY; MWJ and WM analyzed the data. JYG and LWY provided critical materials. C. Yan; WM and C. Yang wrote the manuscript. JYG supervised the study. All the authors have read and approved the final version for publication.

Declaration of Competing Interest

The authors declare that they have no known competing financial interests or personal relationships that could have appeared to influence the work reported in this paper.

Acknowledgments

Thanks for all the contributors and participants.

Funding

This research was funded by the grants from Hunan Provincial Natural Science Youth Foundation (Grant No. 2019JJ50873); Hunan Provincial Health Commission Project Fund (Grant No. 202104040152) and Hunan Provincial Science & Technology Department Planning Project (Grant No. 2018SK21213).

Supplementary materials

Supplementary material associated with this article can be found, in the online version, at doi:10.1016/j.tranon.2021.101282.

References

[1] H.S. Nguyen, S. Shabani, A.J. Awad, M. Kaushal, N. Doan, Molecular Markers of Therapy-Resistant Glioblastoma and Potential Strategy to Combat Resistance, Int. J. Mol. Sci. 19 (6) (2018).
[2] A. Fathi Kazerooni, S. Bakas, H. Saligheh Rad, C. Davatzikos, Imaging signatures of glioblastoma molecular characteristics: a radiogenomics review, J. Magn. Reson. Imaging 52 (1) (2020) 54–69.
[3] M.N. Abbas, S. Kausar, H. Cui, Therapeutic potential of natural products in glioblastoma treatment: targeting key glioblastoma signaling pathways and epigenetic alterations, Clin. Transl. Oncol. 22 (7) (2020) 963–977.
[4] D.M. Park, S. Sathornsumetee, J.N. Rich, Medical oncology: treatment and management of malignant gliomas, Nat. Rev. Clin. Oncol. 7 (2) (2010) 75–77.
[5] A.R. Boileau, F.D. Miller, Changes in spectral sensitivity of multiplier phototubes resulting from changes in temperature, Appl. Opt. 6 (7) (1967) 1179–1182.
[6] P.J. Batista, H.Y. Chang, Long noncoding RNAs: cellular address codes in development and disease, Cell 152 (6) (2013) 1298–1307.
[7] F. Fatima, M. Nawaz, Vesiculated Long Non-Coding RNAs: offshore Packages Deciphering Trans-Regulation between Cells, Cancer Progression and Resistance to Therapies, Noncoding RNA 3 (1) (2017).
[8] G. Ma, M. Tang, Y. Wu, X. Xu, F. Pan, R. Xu, LncRNAs and miRNAs: potential biomarkers and therapeutic targets for prostate cancer, Am. J. Transl. Res. 8 (12) (2016) 5141–5150.
[9] E. Anastasiadou, L.S. Jacob, F.J. Slack, Non-coding RNA networks in cancer, Nat. Rev. Cancer 18 (1) (2018) 5–18.
[10] U. Linz, Aspects on the survival of patients with glioblastoma and the origin and histology of oligodendrogliomas, Nat. Rev. Cancer 3 (7) (2003), https://doi.org/10.1038/nrc1121-c1031.
[11] H. Ding, L. Zhang, C. Zhang, J. Song, Y. Jiang, Screening of Significant Biomarkers Related to Prognosis of Cervical Cancer and Functional Study Based on lncRNA-associated ceRNA Regulatory Network, Comb. Chem. High Throughput Screen. 24 (3) (2021) 472–482.
[12] L. Wang, H. Zhao, Y. Xu, J. Li, C. Deng, Y. Deng, et al., Systematic identification of lincRNA-based prognostic biomarkers by integrating lincRNA expression and copy number variation in lung adenocarcinoma, Int. J. Cancer 144 (7) (2019) 1723–1734.
[13] A. Sanchez-Mejias, Y. Tay, Competing endogenous RNA networks: tying the essential knots for cancer biology and therapeutics, J. Hematol. Oncol. 8 (2015) 30.
[14] A. Kozomara, S. Griffiths-Jones, miRBase: integrating microRNA annotation and deep-sequencing data, Nucleic. Acids. Res. 39 (Database issue) (2011) D152–D157.
[15] M.I. Aslam, M. Patel, B. Singh, J.S. Jameson, J.H. Pringle, MicroRNA manipulation in colorectal cancer cells: from laboratory to clinical application, J. Transl. Med. 10 (2012) 128.
[16] W. Shi, K. Gerster, N.M. Alajez, J. Tsang, L. Waldron, M. Pintilie, et al., MicroRNA-301 mediates proliferation and invasion in human breast cancer, Cancer Res. 71 (8) (2011) 2926–2937.
[17] Z. Liu, L. Chen, X. Zhang, X. Xu, H. Xing, Y. Zhang, et al., RUNX3 regulates vimentin expression via miR-30a during epithelial-mesenchymal transition in gastric cancer cells, J. Cell. Mol. Med. 18 (4) (2014) 610–623.
[18] X. Xia, K. Zhang, G. Cen, T. Jiang, J. Cao, K. Huang, et al., MicroRNA-301a-3p promotes pancreatic cancer progression via negative regulation of SMAD4, Oncotarget 6 (25) (2015) 21046–21063.
[19] A. Santangelo, M. Rossato, G. Lombardi, S. Benfatto, D. Lavezzari, G.L. De Salvo, et al., A molecular signature associated with prolonged survival in glioblastoma patients treated with regorafenib, Neuro. Oncol. 23 (2) (2021) 264–276.
[20] N. Bouche, A. Scharlat, W. Snedden, D. Bouchez, H. Fromm, A novel family of calmodulin-binding transcription activators in multicellular organisms, J. Biol. Chem. 277 (24) (2002) 21851–21861.
[21] Z. He, C. Yang, Y. He, B. Gong, C. Yin, J. Feng, et al., CAMTA1, a novel antitumor gene, regulates proliferation and the cell cycle in glioma by inhibiting AKT phosphorylation, Cell. Signal. 79 (2021), 109882.
[22] K. Ichimura, A.P. Vogazianou, L. Liu, D.M. Pearson, L.M. Backlund, K. Plant, et al., 1p36 is a preferential target of chromosome 1 deletions in astrocytic tumours and homozygously deleted in a subset of glioblastomas, Oncogene 27 (14) (2008) 2097–2108.
[23] V. Barbashina, P. Salazar, E.C. Holland, M.K. Rosenblum, M. Ladanyi, Allelic losses at 1p36 and 19q13 in gliomas: correlation with histologic classification, definition of a 150-kb minimal deleted region on 1p36, and evaluation of CAMTA1 as a candidate tumor suppressor gene, Clin. Cancer Res. 11 (3) (2005) 1119–1128.
[24] D. Schraivogel, L. Weinmann, D. Beier, G. Tabatabai, A. Eichner, J.Y. Zhu, et al., CAMTA1 is a novel tumour suppressor regulated by miR-9/9* in glioblastoma stem cells, EMBO J. 30 (20) (2011) 4309–4322.
[25] T. Yokota, J. Kouno, K. Adachi, H. Takahashi, A. Teramoto, K. Matsumoto, et al., Identification of histological markers for malignant glioma by genome-wide expression analysis: dynein, alpha-PIX and sorcin, Acta Neuropathol. 111 (1) (2006) 29–38.
[26] J. Yang, D. Yu, X. Liu, E. Changyong, S. Yu, LINC00641/miR-4262/NRGN axis confines cell proliferation in glioma, Cancer Biol. Ther. 21 (8) (2020) 758–766.
[27] R. Chen, G.I. Mias, J. Li-Pook-Than, L. Jiang, H.Y. Lam, R. Chen, et al., Personal omics profiling reveals dynamic molecular and medical phenotypes, Cell 148 (6) (2012) 1293–1307.
[28] H. Kim, J.Y. Moon, K.S. Ahn, S.K. Cho, Quercetin induces mitochondrial mediated apoptosis and protective autophagy in human glioblastoma U373MG cells, Oxid. Med. Cell Longev 2013 (2013), 596496.
[29] X. Chen, Z. Chen, S. Yu, F. Nie, S. Yan, P. Ma, et al., Long Noncoding RNA LINC01234 Functions as a Competing Endogenous RNA to Regulate CBFB Expression by Sponging miR-204-5p in Gastric Cancer, Clin. Cancer Res. 24 (8) (2018) 2002–2014.
[30] S. Deguchi, K. Katsushima, A. Hatanaka, K. Shinjo, F. Ohka, T. Wakabayashi, et al., Oncogenic effects of evolutionarily conserved noncoding RNA ECONEXIN on gliomagenesis, Oncogene 36 (32) (2017) 4629–4640.
[31] X. Liu, J. Zheng, Y. Xue, H. Yu, W. Gong, P. Wang, et al., PIWIL3/OIP5-AS1/miR-367-3p/CEBPA feedback loop regulates the biological behavior of glioma cells, Theranostics 8 (4) (2018) 1084–1105.
[32] J. Zheng, X. Liu, P. Wang, Y. Xue, J. Ma, C. Qu, et al., CRNDE Promotes Malignant Progression of Glioma by Attenuating miR-384/PIWIL4/STAT3 Axis, Mol. Ther. 24 (7) (2016) 1199–1215.
[33] K.O. Henrich, M. Fischer, D. Mertens, A. Benner, R. Wiedemeyer, B. Brors, et al., Reduced expression of CAMTA1 correlates with adverse outcome in neuroblastoma patients, Clin. Cancer Res. 12 (1) (2006) 131–138.
[34] M.Y. Kim, S.H. Yim, M.S. Kwon, T.M. Kim, S.H. Shin, H.M. Kang, et al., Recurrent genomic alterations with impact on survival in colorectal cancer identified by genome-wide array comparative genomic hybridization, Gastroenterology 131 (6) (2006) 1913–1924.
[35] G.H. Struijk, A.F. Gijsen, S.L. Yong, A.H. Zwinderman, S.E. Geerlings, K. D. Lettinga, et al., Risk of Pneumocystis jiroveci pneumonia in patients long after renal transplantation, Nephrol. Dial. Transplant. 26 (10) (2011) 3391–3398.

[36] X. Xia, K. Zhang, G. Luo, G. Cen, J. Cao, K. Huang, et al., Downregulation of miR-301a-3p sensitizes pancreatic cancer cells to gemcitabine treatment via PTEN, Am. J. Transl. Res. 9 (4) (2017) 1886–1895.
[37] J. Wang, L. Tan, L. Tan, Y. Tian, J. Ma, C.C. Tan, et al., Circulating microRNAs are promising novel biomarkers for drug-resistant epilepsy, Sci. Rep. 5 (2015) 10201.
[38] M.I. Kester, C.E. Teunissen, D.L. Crimmins, E.M. Herries, J.H. Ladenson, P. Scheltens, et al., Neurogranin as a Cerebrospinal Fluid Biomarker for Synaptic Loss in Symptomatic Alzheimer Disease, JAMA Neurol. 72 (11) (2015) 1275–1280.
[39] A.O. Koob, G.M. Shaked, A. Bender, A. Bisquertt, E. Rockenstein, E. Masliah, Neurogranin binds alpha-synuclein in the human superior temporal cortex and interaction is decreased in Parkinson's disease, Brain Res. 1591 (2014) 102–110.
[40] K. Ohi, R. Hashimoto, Y. Yasuda, M. Fukumoto, H. Yamamori, S. Umeda-Yano, et al., Influence of the NRGN gene on intellectual ability in schizophrenia, J. Hum. Genet. 58 (10) (2013) 700–705.
[41] J.M. Lamar, V. Motilal Nehru, G. Weinberg, Epithelioid Hemangioendothelioma as a Model of YAP/TAZ-Driven Cancer: insights from a Rare Fusion Sarcoma, Cancers (Basel) 10 (7) (2018).
[42] C.N. Seavey, A.V. Pobbati, A. Hallett, S. Ma, J.P. Reynolds, R. Kanai, et al., WWTR1 (TAZ)-CAMTA1 gene fusion is sufficient to dysregulate YAP/TAZ signaling and drive epithelioid hemangioendothelioma tumorigenesis, Genes Dev. 35 (7–8) (2021) 512–527.
[43] Z. Liu, Y. Wei, L. Zhang, P.P. Yee, M. Johnson, X. Zhang, et al., Induction of store-operated calcium entry (SOCE) suppresses glioblastoma growth by inhibiting the Hippo pathway transcriptional coactivators YAP/TAZ, Oncogene 38 (1) (2019) 120–139.
[44] K. Vigneswaran, N.H. Boyd, S.Y. Oh, S. Lallani, A. Boucher, S.G. Neill, et al., YAP/TAZ Transcriptional Coactivators Create Therapeutic Vulnerability to Verteporfin in EGFR-mutant Glioblastoma, Clin. Cancer Res. 27 (5) (2021) 1553–1569.
[45] L. Zhang, F. Cheng, Y. Wei, L. Zhang, D. Guo, B. Wang, et al., Inhibition of TAZ contributes radiation-induced senescence and growth arrest in glioma cells, Oncogene 38 (15) (2019) 2788–2799.